systems

MDPI

Article

Augmenting Process Failure Mode and Effects Analysis with Fuzzy Cognitive Mapping for Dynamic Manufacturing Risk Assessment

Amin Sehati [1,*] and Steven A. Gray [2,*]

[1] College of Graduate and Professional Studies, Trine University, Allen Park, MI 48101, USA
[2] Department of Community Sustainability, Michigan State University, East Lansing, MI 48824, USA
* Correspondence: amin@aminsehati.com (A.S.); stevenallangray@gmail.com (S.A.G.)

Highlights

Please indicate how your work links to systems science via your contributions to systems practice, theory, and/or methodology.

- The study links local failure assessment to the behavior of the wider manufacturing system through Fuzzy Cognitive Mapping.
- The framework offers a way to apply systems thinking within established PFMEA practice without changing the PFMEA worksheet.

What are the main findings and/or the implications of the main findings?

- In the illustrative case, ranking actions by modeled risk reduction replaces one of the three actions prioritized by RPN; the top-three set among shared failure modes remains unchanged across tested perturbations.
- Throughput pressure and fatigue emerge as intervention targets even though the PFMEA worksheet records them only as causes.

Abstract

Conventional Process Failure Mode and Effects Analysis (PFMEA) is linear and does not explicitly include a systems-based perspective that accounts for the complexity in which all manufacturing systems operate. In an illustrative case study using hypothetical inputs, this study augments traditional PFMEA methods with a Fuzzy Cognitive Mapping (FCM) approach. We suggest a Leverage Impact Number (LIN) that quantifies modeled system-wide risk reduction to include the impacts of individual intervention options available to decision-makers to better quantify risk, but also the relative contribution of management intervention to reduce those risks. Rank comparisons examine changes in priorities and an analysis of concepts covered only by the FCM considers organizational factors. Monte Carlo perturbations assess sensitivity to causal weights, and one-way analyses examine risk weighting, mitigation levels, driver baselines, transfer-function steepness, and the update rule. When traditional PFMEA is compared with our FCM-augmented approach, our results indicate that LIN and Risk Priority Number (RPN) rankings are moderately correlated in this illustrative case, with the augmented approach retaining key PFMEA priorities while extending the analysis to modeled system-wide intervention effects. Under reference assumptions, combined stressors increase modeled risk by approximately the sum of their separate effects. These results demonstrate additional decision support information under the same stated assumptions when using PFMEA and our FCM-augmented method.

Check for updates

Academic Editor: Zaoli Yang

Received: 8 August 2026
Revised: 27 September 2026
Accepted: 8 October 2026
Published: 16 October 2026

Copyright: © 2026 by the authors. Licensee MDPI, Basel, Switzerland. This article is an open access article distributed under the terms and conditions of the Creative Commons Attribution (CC BY) license.

Keywords: process failure mode and effects analysis; fuzzy cognitive maps; manufacturing risk assessment; leverage points; Action Priority; risk prioritization; Industry 4.0

1. Introduction

Failure Mode and Effects Analysis (FMEA) is one of the most frequently used techniques in quality management and failure analysis. As the name suggests, the method establishes and standardizes a common language and specific dimensions for systematic analysis of potential failure modes, as well as the causes and effects of the corresponding failures [1,2]. The objective of FMEA is to minimize the risks of failure and to create an understanding of what preventive actions or corrective actions can prevent failures from reaching the customer, especially when developing new products or processes [3]. Process FMEA, as a specific type of FMEA, is commonly used to assess potential failure modes within a manufacturing process that may result in a product that does not meet specified requirements [4]. The analysis is recorded in a PFMEA worksheet, a structured table in which each row links a process step and work element to its function, failure mode, failure effect, and failure cause, together with the current prevention and detection controls and the severity, occurrence, and detection ratings used to prioritize action [2]. The worksheet serves as the auditable record of the analysis. In 2019, the Automotive Industry Action Group (AIAG) and Verband der Automobilindustrie (VDA) published a harmonized FMEA handbook to provide a common methodology for automotive manufacturers and their international suppliers [2]. This AIAG-VDA revision replaced the multiplicative metric of Risk Priority Number (RPN) with a severity-first Action Priority (AP) classification with High, Medium, or Low as the basis for action. As a largely qualitative and subjective risk management approach, PFMEA is a widely recognized tool in various industries that involve manufacturing. For example, it is often seen as a normative tool in the automotive industry among Original Equipment Manufacturers (OEMs) and suppliers allowing for a shared methodology for international production of parts. Additionally, in the medical device sector PFMEA is increasingly applied as a practical risk-analysis tool for risk-based quality management to support alignment with US Food and Drug Administration expectations and ISO 13485 [5], the internationally recognized standard for Quality Management Systems (QMS) in the medical device industry [6].

Although extremely useful for international standardization, PFMEA is constrained by several limitations which have been identified, including the following: subjectivity of severity, occurrence, and detection ratings; ambiguities in cause and effect relationships; and the practical aspects of managing the data and keeping it up to date [7]. Further, traditional PFMEA examines failure mode in isolation when failures can certainly be attributed to system dynamics not accounted for in the assessment. That means when multiple failures coincide in a complex system, it might not capture all failure interactions due to the degree of interdependency within processes. Although a PFMEA can be revised as processes change, the PFMEA worksheet itself does not simulate the propagation of an imposed change through a causal network. Short product lifecycles and changing manufacturing processes [8] motivate such conditional analysis. Here, "dynamic" refers to propagation between modeled steady states compared to continuous updating from factory data as production continues under changing conditions. To overcome some of the limitations of traditional FMEA scoring, many researchers have suggested adding nuances through using fuzzy sets and multi-criteria decision methods to improve failure mode assessments [9]. Fuzzy extensions add measurement fidelity by allowing severity, occurrence, detection, and, where applicable, additional risk factors to be evaluated through linguistic terms

represented by fuzzy membership functions rather than integer scores. Therefore, the imprecision and variability inherent in expert judgment are represented rather than discarded [10,11]. The multi-criteria decision-making (MCDM) layer adds decision structure by permitting criteria or risk factors to receive unequal, explicitly derived weights. Accordingly, the problem of indistinguishable rankings from equal-weight multiplication in conventional RPN calculation is somewhat addressed by aggregating the resulting evaluations through systematic ranking procedures [10–12]. Their combined value consequently lies in achieving a more nuanced representation of individual judgments and a more transparent and defensible aggregation into priorities. The failure modes themselves, however, are scored as separate items in these extensions, which therefore leaves the causal structure that links them somewhat uncertain for decision-makers.

FMEA was formalized in United States military reliability procedures in 1949 through MIL-P-1629 [13]. Since then, manufacturing has undergone substantial change, including the networked digitalization and automation associated with Industry 4.0 [14]. Thomas [15] argues that FMEA needs to adapt to a manufacturing landscape known for its rapid technological change and complex supply chains. Research on digital technologies and supply-chain risk similarly emphasizes the propagation of disruptions through interconnected systems [16]. Recent FMEA work on collaborative robots highlights the need to consider human and psychosocial factors alongside technological hazards [17]. Although human and organizational conditions can be recorded as causes in a PFMEA worksheet, the worksheet does not explicitly model their feedback relationships or quantify their system-wide intervention effects. Complementary work on manufacturing fault diagnosis uses logical and probabilistic models to identify possible fault origins and support corrective maintenance decisions [18]. These developments motivate supplementing local failure assessments with explicit analysis of interactions, feedback, and risk propagation among technical, human, and organizational factors.

Traditional PFMEA also has difficulty representing cascading or systemic failures arising from interactions between interconnected process steps and stations. It lacks a systematic method to capture failures that originate at one point in the process and propagate downstream across the entire production flow. Driven by the Internet of Things (IoT), machine learning, and artificial intelligence, the evolution of discrete manufacturing steps into data-integrated, tightly coupled process chains has significantly altered the risk assessment landscape and complicated root cause analysis [14]. Although such technologies improve monitoring and control, they also deepen the interconnectivity through which a failure at one step propagates downstream. This highlights the role of risk propagation, an effect that conventional PFMEA's isolated scoring fails to capture.

1.1. Fuzzy Cognitive Mapping

Fuzzy Cognitive Maps (FCMs) are semi-quantitative network representations comprised of causal structures of a system. Originally developed by Kosko [19], FCMs combine cognitive mapping with fuzzy mathematics by representing systems as directed graphs composed of concepts (nodes) connected by weighted causal relationships. Concepts may include technical, organizational, behavioral, environmental, or operational factors as long as they can increase or decrease in quantity or quality, while connections indicate the direction and relative strength of an influence between them. Positive links indicate that an increase in one variable is expected to increase another, while negative links indicate that an increase in one variable is expected to decrease another. These maps can be converted into adjacency matrices, analyzed using graph-theoretic measures, aggregated and used to run "what-if" scenarios that estimate how changes in one part of a system may propagate through the larger network [19–21].

FCMs have been widely used across disciplines such as environmental management, social-ecological systems research, futures studies, risk analysis, and decision support because they provide a structured way to make expert and stakeholder knowledge explicit [21,22]. In these research contexts, FCMs are especially useful when systems are complex, data are incomplete, and multiple forms of knowledge need to be integrated. Özesmi and Özesmi [20] demonstrated how FCMs could be used to model ecological systems based on expert and local knowledge as well as to compare stakeholder understandings. Similarly, Gray et al. [23] used FCMs to examine differences and similarities in stakeholder mental models in fisheries governance, showing how FCMs can characterize both the structure and function of knowledge across groups. More broadly, FCMs have been used to support participatory modeling and scenario analysis in systems where uncertainty and feedback are central features of the problem [22].

Fuzzy logic has a well-established record in manufacturing and reliability engineering. Reviews document its application across a broad range of manufacturing and production decisions, from the progression of fuzzy tools in manufacturing decisions over two decades [24] to a survey of fuzzy set theory in production and operations management from 1998 to 2009 [25]. In reliability engineering, an early fuzzy-logic framework for prioritizing failure modes within a Failure Mode, Effects and Criticality Analysis (FMECA) addresses the limitations of conventional FMEA methods that rely on numerical scoring for severity, occurrence, and detectability [26]. FCMs complement these approaches by representing concepts and their weighted causal relationships as a dynamic system. For example, FCMs have been investigated for supervisory control of manufacturing systems [27,28] and for assessing factors affecting operator reliability in production systems [29].

Other applications include modeling industrial processes, illustrated by a heat exchanger [30]. Reviews survey FCM applications across multiple domains [31] and developments in learning methods and implementation software [32]. In reliability engineering, Salmeron and Gutierrez [33] combine fuzzy gray cognitive maps with failure analysis to model relationships among transformer failure causes and simulate failure scenarios. Bakhtavar et al. [34] review industrial safety and reliability applications, including FMEA–FCM approaches to occupational risk in manufacturing and PFMEA–FCM approaches to process-risk prioritization.

Several primary studies directly combine PFMEA with multi-stage cognitive maps. Jahangoshai Rezaee et al. [35] developed a multi-stage map and learning algorithm for prioritizing failures in automotive-parts production using severity, occurrence, detection, and causal relationships. Their subsequent food-production study [36] considers relationships within and between process stages when calculating failure-prioritization scores. Yousefi et al. [37] combine PFMEA with a sequential multi-stage FCM to prioritize logistics risks in an automotive spare-parts company. Abbaspour Onari et al. [38] extend multi-stage FCM risk assessment with Z-numbers and a fuzzy learning algorithm to represent uncertainty and reliability in automotive-parts production. These studies establish a basis for using causal maps in manufacturing failure analysis; Section 1.2 specifies the intervention-comparison workflow examined here.

In manufacturing risk assessment, FCMs can be a particularly helpful methodology because they can represent forms of causal complexity that are difficult to capture in conventional FMEA. Traditional FMEA approaches typically identify failure modes, causes, effects, and controls, then rank risks using severity, occurrence, and detection scores. Research on FMEA deployment in complex systems identifies difficulties in tracing failure effects and coordinating analyses and supports the use of complementary methods [39]. FCMs provide a complementary systems-analysis layer by linking failure modes, process conditions, controls, human factors, machine states, and quality outcomes in a dynamic

causal model. Peláez and Bowles [40] explicitly proposed FCMs as system models for FMEA, using their directed causal structure to predict the effects of component failures on complex-system operation. The present study builds on this established use of FCMs in failure analysis; its specific contributions are stated in Section 1.2.

1.2. Research Gap and Contributions

This paper develops a workflow for augmenting PFMEA with FCM and demonstrates its use in an illustrative manufacturing case (Figure 1). The aim is to make intervention effects, organizational relationships, and conditional scenario responses available alongside the PFMEA worksheet's existing priorities. The comparison evaluates these methodological capabilities; validation against production outcomes is a subsequent step.

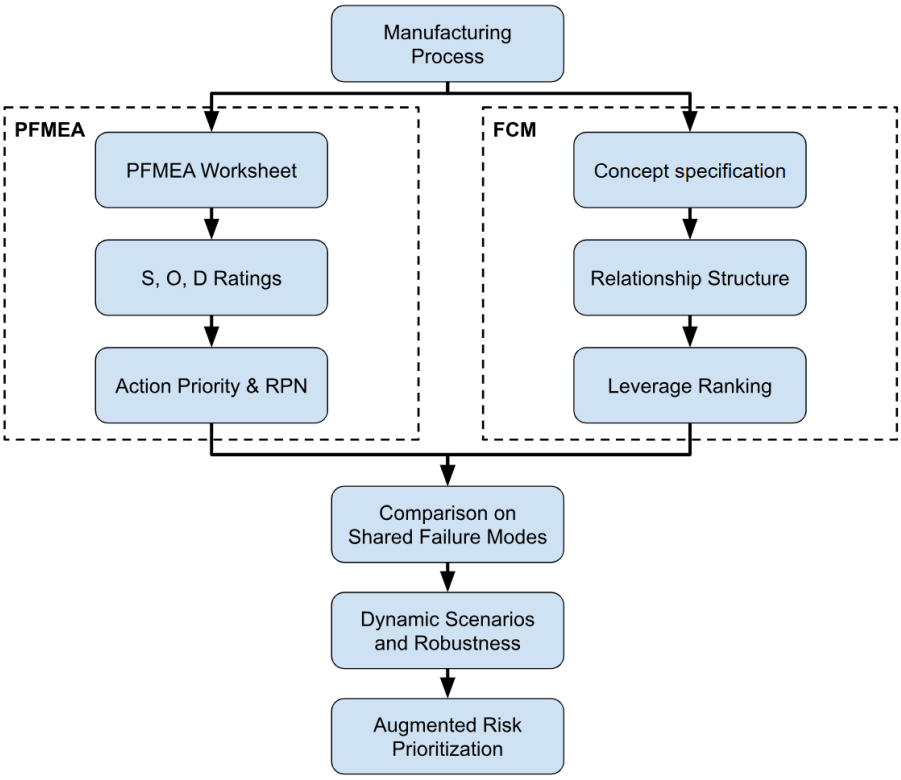


Figure 1. Research framework of the proposed methodology.

We suggest that the value of FCMs is in augmenting and extending PFMEA and not replacing established quality-management routines [9]. PFMEA provides a disciplined and standardized framework for identifying potential failures and prioritizing corrective actions while FCMs add the ability to represent interdependencies among those failures, visualize system-wide causal pathways, and simulate how changes in process conditions or controls may alter risk. This makes FCMs especially appropriate for modern manufacturing environments characterized by several interacting subsystems including automation, digitalization, human–machine interaction, tightly coupled process steps, and increasingly dynamic operating conditions. In an FCM-augmented PFMEA, the risk assessment can move from a static table-based assessment toward a causal systems model that makes causal assumptions explicit and supports scenario-based decision making for process reliability and operational resilience. Connecting such a model to real-time or periodically updated factory data is a further step that this paper motivates but does not implement (see Section 5).

The practical question is what the augmentation adds to decisions based on PFMEA worksheet ratings: the estimated effect of a specified mitigation, the role of an organizational

condition across several failure modes, and the response to combined stressors. These are additions to the PFMEA decision process; a different or more detailed ranking does not by itself establish which actions should be implemented.

To illustrate this workflow, we develop a manufacturing case study involving an automated assembly process. In our case study, the baseline PFMEA documents seven failure modes: (1) operator part-loading error, (2) sensor drift, (3) force-window mis-setting, (4) press-tooling wear, (5) out-of-window insertion depth, (6) missed in-line detection, and (7) supplier component variability. The S, O, and D ratings are hypothetical values using the AIAG-VDA rating scales (Section 3.7). These ratings are used to calculate baseline RPN values and determine Action Priority classes for each failure mode. The same case is then modeled using FCM to represent causal links among the failure modes and operating conditions. The FCM also represents three organizational conditions not independently rated in the worksheet: throughput pressure and operator fatigue, maintenance backlog and rework, and maintenance budget adequacy. Throughput pressure and operator fatigue appear in the PFMEA worksheet only as unrated cause text.

We conduct a comparative analysis of PFMEA alone and PFMEA supported by FCM. The PFMEA worksheet is retained unchanged as the baseline, and the FCM represents the seven shared failure modes alongside additional operating conditions and outcomes. Its concepts and weights were set by the authors as hypothetical modeling assumptions (Section 3.7). Intervention comparisons within Action Priority bands, an analysis of concepts covered only by the FCM (labeled FCM-only in Table 1), and conditional what-if scenarios demonstrate the additional decision information. The RPN–LIN rank comparison identifies retained and changed priorities, while sensitivity analyses examine dependence on the tested assumptions. All numerical results relate to a hypothetical manufacturing cell and are not validated against observed defect rates, downtime, or intervention outcomes.

Table 1. Concept inventory. FCM role denotes the analytical function (driver = clamped exogenous input; state = free concept; outcome = read into the composite risk). A concept is "shared" when it corresponds one to one with a rated failure-mode row of the PFMEA worksheet (Table A1); it is "FCM-only" when it appears in the worksheet only as unrated effect or cause text, or not at all (Section 4.4, Table A3).

ID	Concept	FCM Role	In PFMEA?
C1	Force/displacement sensor drift	state	shared
C2	Press force-window calibration error	state	shared
C3	Press tooling wear	state	shared
C4	Insertion force out of range	state	shared
C10	Operator loading error	state	shared
C11	Supplier component variability	driver	shared
C13	In-line inspection effectiveness	state	shared
C5	Press-fit joint defect rate	outcome	FCM-only
C14	Downstream e-drive escaped failure	outcome	FCM-only
M1	Throughput pressure & operator fatigue	state	FCM-only
M2	Maintenance backlog and rework	state	FCM-only
C8	Maintenance budget adequacy	driver	FCM-only

Previous related studies [40] used FCMs to predict the effects of component failures, while later PFMEA–FCM studies prioritize failures or risks using scores that incorporate causal dependencies [35–37]. Uncertainty-aware extensions also account for the reliability of risk-factor values and causal weights [38]. Combining PFMEA with FCM, retaining a PFMEA worksheet, and assigning per-concept scores are not necessarily completely novel. Some previous studies have emphasized failure-prioritization scores and learning from risk-factor information. However, this study evaluates the fixed-point reduction

in a common risk objective from separately clamping each intervention candidate. Our contribution is the comparison of these intervention effects within retained AIAG-VDA Action Priority bands, together with sensitivity to the chosen risk weighting, clamp levels, driver baselines, transfer-function steepness, and update rule.

The workflow combines five elements: (1) retention of the PFMEA worksheet and its AIAG-VDA Action Priority classifications, preserving compliance and audit artifacts; (2) the development of a Leverage Impact Number (LIN), defined as the percentage reduction in modeled composite risk from mitigating each candidate factor separately relative to a common baseline, for comparing intervention leverage within Action Priority bands; (3) rank-agreement analysis on shared failure modes and analysis of concepts covered only by the FCM, which are not independently rated in the PFMEA worksheet; (4) clamped what-if scenarios with an additivity diagnostic to compare combined and separate stressor effects; and (5) including sensitivity analysis of causal weights, modeling constants, transfer-function steepness, and update rule, identifying both stable conclusions and limits. The workflow is demonstrated on an illustrative automotive e-drive press-fit cell using hypothetical inputs.

2. Case Study: Press-Fit Assembly in Automotive E-Drive Manufacturing

The case study selected for this analysis is an automotive e-drive press-fit assembly cell with sensor-driven force control, in-line inspection, planned maintenance, and variable supplier inputs. A press-fit joint is formed by forcing one component into a dimensionally interfering mate and producing interface contact pressure and friction that retain the components without a separate fastener, adhesive, or weld. In an electric-drive (e-drive) unit, the integrated motor and gearbox assembly of an electric vehicle, such joints secure bearings, shafts, and housings that must survive high torque, vibration, and thermal cycling over the vehicle's life. The studied cell brings together the subsystems typical of modern powertrain assembly: a press with closed-loop force control, force and displacement sensors with calibrated acceptance windows, press tooling, operator part loading, in-line inspection, planned maintenance, and a stream of supplier-provided components (Figure 2).

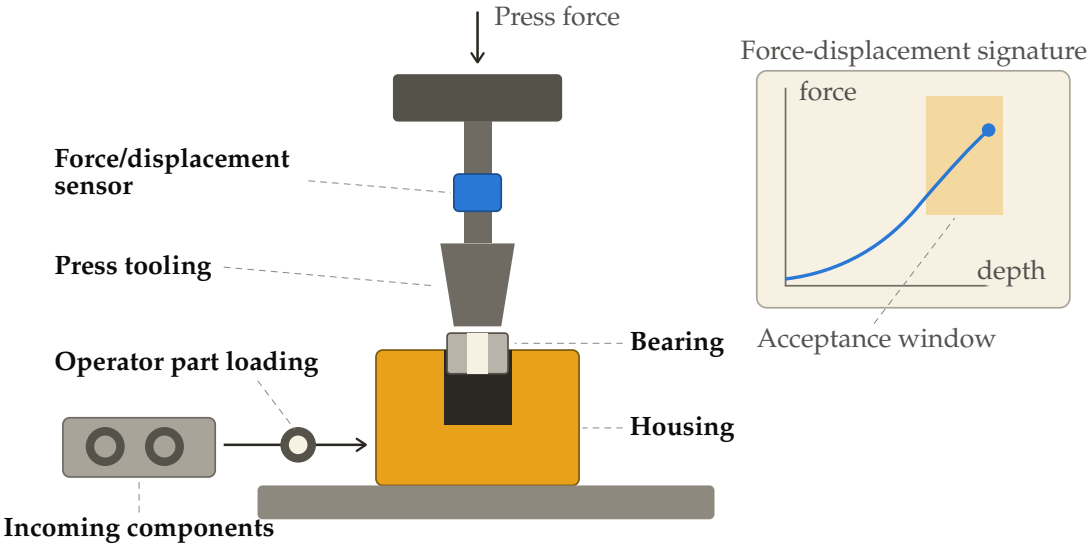


Figure 2. Schematic of the press-fit assembly cell: the sensor-equipped press seats a bearing into the e-drive housing, with operator part loading, incoming components, and the force-displacement signature monitored against its acceptance window.

What makes the process demanding is that joint quality is not directly observable after assembly; it is inferred from the force-displacement signature recorded during insertion,

so the measurement chain of sensors, calibration, and acceptance windows is itself a potential failure source alongside the mechanics [41] (Figure 3). The consequences can lead to insufficient interference or misalignment and therefore loosening and noise in service; whereas excessive force damages bearings or housings, and a defective joint that escapes detection surfaces only later as a costly field failure of the e-drive. Hence, the cell is an instructive case for risk methodology: technical, human, and organizational factors, from tooling wear and operator loading under time pressure to maintenance funding and supplier variation, interact through feedback rather than in isolation, which is precisely the structure a PFMEA worksheet-based analysis struggles to represent. Two complementary analyses of this cell are developed: a conventional PFMEA that establishes the standards-compliant baseline, and a Fuzzy Cognitive Map that augments it.

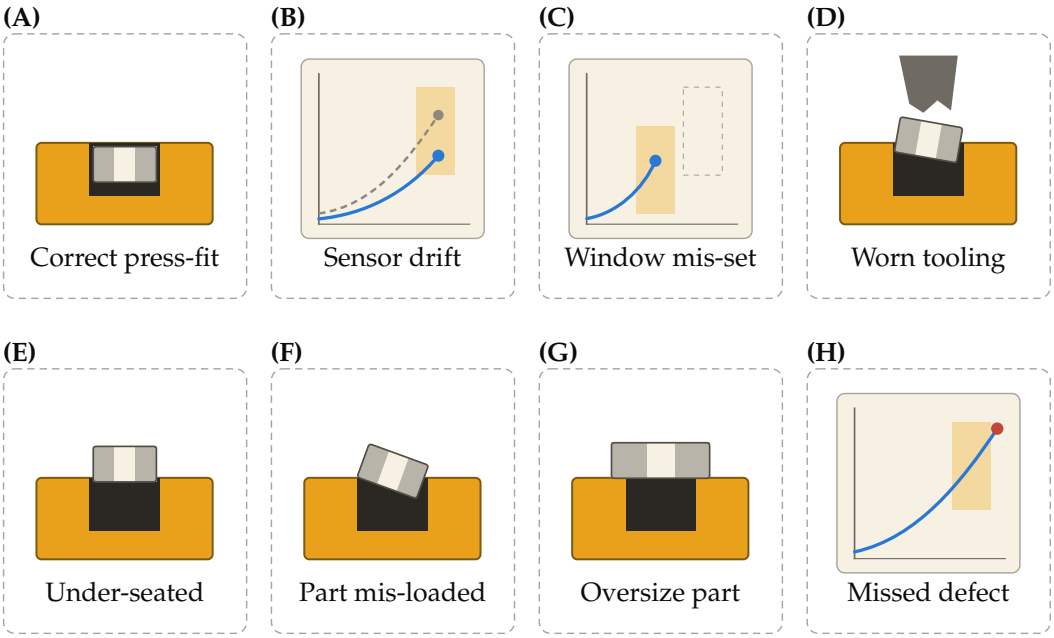


Figure 3. (**A**) Correct press-fit joint (reference, not a failure mode) and (**B**–**H**) the seven failure modes that form the PFMEA worksheet rows of Table A1. Measurement-chain failures on the signature: (**B**) sensor drift; (**C**) window mis-set = force-window mis-setting; (**H**) missed defect = missed in-line detection. Physical failures at the bore: (**D**) worn tooling = press tooling wear; (**E**) under-seated = insertion depth out of window; (**F**) part mis-loaded = operator part-loading error; (**G**) oversize part = supplier component variability.

3. Materials and Methods

3.1. Creating PFMEA Baseline

To construct a baseline against which the augmented approach can be compared, the scope of the automotive manufacturing process is first established and the failure modes within it are identified; these are then rated and prioritized to provide a quantitative basis for comparison. Each failure mode is evaluated using three core criteria: severity (S), which measures the impact of the failure; occurrence (O), which represents the likelihood of its cause; and detection (D), which rates the effectiveness of current controls in catching the failure. To determine the urgency of corrective actions, Action Priority (AP) classification is used as the current AIAG-VDA decision basis at the time of this study to prioritize risk. AP, taking the values Low, Medium, and High, is obtained from the Action Priority Evaluation Table [2]. AP is reported alongside RPN for conformance with the current AIAG-VDA standard. RPN provides more distinct values among the seven shared failure modes in this case and is therefore used for the principal rank comparison with LIN. AP is also compared with LIN using a rank correlation adjusted for shared ranks, while recognizing

the limited discrimination of its three categories. Neither comparison treats differences between ordinal ratings or AP categories as equal numerical intervals.

3.2. Fuzzy Cognitive Map Architecture

3.2.1. FCM Structure and Composition

The automotive process under study is modeled as a Fuzzy Cognitive Map consisting of n concepts, each with activation A_i, and a weighted adjacency matrix W, where $w_{j\to i} \in [-1, 1]$ represents the influence of concept j on concept i [42]. Structurally, transmitter concepts influence other concepts but have no incoming edges, receiver concepts have incoming but no outgoing edges, and ordinary concepts have both. The drivers in this model are transmitters whose activations are held fixed during a run. The term "outcome" instead denotes an analytical role: an outcome is a concept included in the composite risk score and need not be a structural receiver. Thus C5 can contribute to composite risk while also transmitting effects to other concepts, as explained in Section 4.2.

3.2.2. FCM Dynamics and Scenarios

FCMs can be used to understand dynamic scenarios by simulating how changes propagate through the causal weights and network structure of a model. Activations are normalized to $(0, 1)$ by a logistic transfer with 0.5 as the neutral reference, and should be interpreted as relative levels instead of actual units attached to any concept. We use the memoryless Kosko rule to update the activation functions synchronously as follows:

$$A_i(t+1) = f\left(\sum_j w_{j\to i}\, A_j(t)\right), \qquad f(x) = \frac{1}{1+e^{-\lambda x}}, \qquad \lambda = 1 \quad \text{(reference value)}. \tag{1}$$

where $A_i(t) \in (0, 1)$ is the activation of concept i at iteration t, f is the logistic transfer function, and $\lambda > 0$ is the steepness parameter.

Because the update rule has no self-memory or bias term, absolute activation values are implementation-specific, and interpretation focuses on rankings and directional responses. The memoryless rule is used instead of the self-memory ("modified Kosko") variant [43] for two reasons. First, driver concepts are re-clamped at every iteration, so a memory term is not needed to maintain exogenous conditions. Second, a self-memory term adds inertia that the causal weights do not encode, so a concept's response would no longer reflect the specified edges alone. The self-memory variant, $A_i(t+1) = f\Big(A_i(t) + \sum_j w_{j\to i} A_j(t)\Big)$ with the same clamps, is tested as a sensitivity case in Section 4.6.

The model is run until concept values stabilize, while prescribed driver, intervention, and scenario values remain fixed. Results describe these settled conditions rather than intermediate changes. Checks using different starting values produced consistent results for the conditions tested. Supplementary Material S1 provides the implementation and numerical checks.

3.3. Composite Risk Definition

In this study, composite risk is calculated from the fixed-point (steady-state) activations of the internal joint-defect outcome C5 and the downstream escaped-failure outcome C14, with the latter assigned 2.5 times the weight of the former:

$$R = A^*_{\mathrm{C5}} + 2.5\, A^*_{\mathrm{C14}}, \tag{2}$$

where $A^*_i = A_i(t)$ denotes the activation of concept i at the converged fixed point of Equation (1) under the stated clamps.

The outcome concepts of focus in an FCM are aggregated into a composite risk score, calculated as a weighted sum of their steady-state activation levels. Outcomes representing failures that reach the field are assigned larger weights than those contained internally. Treating the aggregate objective as a weighted sum follows standard multi-attribute practice [44], and the weight ordering follows the cost-of-quality principle that external failure costs (warranty, field repair, reputational loss) exceed internal failure costs (scrap, rework). The ratio of 2.5:1 used in this study encodes that ordering with a margin large enough to make the escaped-failure outcome dominant without making the internal defect rate negligible; it is a modeling constant, not a measured cost ratio. The tested ratios from 1:1 to 10:1 retain the same LIN ordering of the seven shared failure modes (see Section 4.6); this does not imply an unchanged ordering of all ten non-outcome concepts. A practitioner adapting the framework should set the ratio from the plant's own cost-of-quality accounting (for example, the ratio of average external to internal failure cost per defect) and repeat the one-way sensitivity analysis of Section 4.6. Each concept is additionally assigned a polarity with respect to the composite risk. A negative concept is one whose increased activation raises the risk, and a positive concept is one whose increased activation reduces it. It should be noted that the polarity qualifies the concept's relation to the risk objective, not the sign of any edge. The leverage of a concept shows how much the system's total risk decreases when that concept alone is clamped in its risk-mitigating direction. A concept whose improvement results in a large reduction constitutes a leverage point of the system. This leverage point is an intervention target at which a local mitigating action propagates into system-wide risk reduction. LIN is evaluated for the ten non-outcome concepts; the two outcome concepts define the objective rather than serving as intervention candidates. For each potential intervention, the target concept is clamped to its mitigation value. All other drivers remain at their baseline values, and the remaining concepts evolve iteratively. If the target is itself a driver, its mitigation clamp replaces its baseline clamp. The model is re-solved to its new fixed point, and the resulting risk is compared with the baseline risk through the Leverage Impact Number (LIN),

$$\mathrm{LIN}(C) = \frac{R_0 - R_C}{R_0} \times 100\%, \tag{3}$$

where C denotes the individual concept under evaluation, R_0 represents the composite risk at the unperturbed baseline steady state, and R_C denotes the composite risk at the post-intervention fixed point, with R evaluated from fixed-point activations as in Equation (2). The resulting ratio expresses the reduction in composite risk as a percentage of the baseline value and compares the effects of the specified target levels. It does not normalize for the size or cost of each intervention. In this study, a negative concept is clamped to 0.15 and a positive concept to 0.85 for the intervention scenario. These values are illustrative target levels on the activation scale, relative to the assumed neutral value of 0.5: 0.15 denotes a low level of a risk-raising concept (for example, little tooling wear), and 0.85 a high level of a risk-reducing concept (for example, highly effective inspection). The targets lie symmetrically 0.35 from the neutral value of 0.5, although the change from baseline differs between concepts. They stay away from the scale limits of 0 and 1, which would represent complete elimination or perfect performance rather than a practical mitigation. Both targets lie beyond the baseline activation of every state concept in its mitigating direction (see Section 4.2), and Table A4 shows that the order of the seven shared modes is unchanged for clamp pairs from 0.05/0.95 to 0.15/0.85. For a driver concept the mitigation clamp is applied on the activation scale, not relative to the driver's baseline, so the leverage of a driver that already sits at a favorable operating point (C11 at 0.20, C8 at 0.80) reflects only the short distance from that baseline to the clamp. These distances differ from the larger changes imposed on free state concepts (concepts not changed for scenarios), so the LIN

ordering is conditional on the intervention targets rather than a comparison of equal-sized improvements. A target equal to the baseline produces zero LIN; a target beyond the baseline in the adverse direction is not a mitigation and can produce negative LIN. This applies to both C11 and C8 in the sensitivity analysis. The results of using a driver clamp as a leverage point are reported for C11 in Table 2 and for C8 in Table A3, but the influence of drivers on composite risk is assessed primarily through the degradation scenarios of Section 3.5, in which C11 emerges as the most influential single stressor at the reference settings. Accordingly, every relative effect reported in this study is a comparison between two fixed points. A mitigating intervention or a degraded scenario condition moves the model to a new fixed point, whose composite risk is compared with that of the baseline steady state [19].

Table 2. PFMEA (Action Priority and legacy RPN) versus the FCM Leverage Impact Number for shared failure modes.

Failure Mode	RPN	RPN Rank	AP	Leverage Impact Number (%)	LIN Rank
C3 Press tooling wear	175	1	M	3.43	2
C13 In-line inspectioneffectiveness	162	2	M	9.54	1
C4 Insertion force out of range	160	3	M	0.32	5
C2 Force-window calibration error	126	4	M	0.04	6
C11 Supplier component variability	120	5	L	0.38	4
C10 Operator loading error	112	6	M	3.36	3
C1 Force/displacement sensor drift	90	7	L	0.01	7

3.4. Rank Agreement Between PFMEA and FCM Prioritization

The comparative analysis examines intervention priorities on the seven shared failure modes, concepts covered only by the FCM, and conditional stressor responses. Monte Carlo and one-way sensitivity analyses examine the dependence of these results on the tested assumptions.

RPN and LIN are not comparable as scales: they measure different things on different scales, but both provide qualitative ordinal rankings, so only their rankings are compared. RPN is the product of three ordinal ratings assigned to a failure mode in isolation, whereas LIN is the percentage reduction in composite risk obtained when that mode is mitigated inside the causal network. Both can inform prioritization of the same seven failure modes, but they express different decision criteria, so the comparison is made on ranks only. The rank comparison identifies which priorities are retained from the PFMEA worksheet and which change under the modeled intervention criterion. It provides context for the intervention comparison (Section 4.3), concepts covered only by the FCM (Section 4.4), and conditional scenarios (Section 4.5). These analyses demonstrate the additional decision information provided under explicit causal assumptions. Agreement or divergence does not establish that either ordering leads to better production decisions. Agreement is quantified by the Spearman rank correlation between RPN and Leverage Impact Number [45], calculated as

$$\rho = 1 - \frac{6\sum_{i=1}^{N} d_i^2}{N(N^2-1)}, \tag{4}$$

where ρ is the rank correlation coefficient ranging from $+1$ indicating exactly similar ordering to -1 meaning opposite ordering, d_i is the difference between the order associated with the i-th shared failure mode between PFMEA and FCM, and N is the total number of shared failure modes. Equation (4) assumes that no two modes share the same rank. When modes share a rank (tied ranks), as under Action Priority, ranks are replaced by mid-ranks and the coefficient is computed as the Pearson correlation of the mid-ranks, which is the

Spearman coefficient adjusted for shared ranks. A supplementary comparison excludes C11, the only driver among the shared modes, to show how the reference result changes for the six shared state concepts. The coefficient describes the seven shared modes in this illustrative case. For statistical context, we also report an exact permutation p-value over all $7! = 5040$ orderings and an approximate 95% confidence interval using the Fisher z transformation with the standard error of Bonett and Wright [46]. These summaries rely on their statistical reference assumptions; they do not quantify uncertainty in the hypothetical inputs or validate intervention outcomes. Sensitivity to the modeling assumptions is examined separately in Section 3.6.

3.5. Concepts Covered Only by the FCM and Dynamic Scenario Analyses

Two features of the FCM augmentation are examined: analysis of concepts not independently rated in the PFMEA worksheet, and what-if scenarios based on explicit causal propagation. The analysis identifies which FCM concepts have corresponding rated failure modes, which appear only in PFMEA worksheet cause or effect text, and which are additional to the worksheet. Their relative influences within the causal network are then examined. This comparison concerns the supplied PFMEA worksheet; it does not imply that PFMEA can never record these factors.

In this paper, "dynamic" means that an imposed change propagates through the causal network until the model reaches a new steady state. Each scenario result compares two fixed points. The term does not mean updating the model in real time from factory data (which we discuss for future work). The scenario analysis clamps selected stressor concepts (drivers C8 and C11 and non-driver concept M1) to prescribed scenario values, one at a time and together. A scenario clamp holds the selected concept at its scenario value at every iteration. For the drivers C8 and C11, this value replaces their baseline clamp; for M1, it replaces the value the model would otherwise compute (0.55 at baseline). Drivers that are not part of a scenario keep their baseline values, and all unclamped non-driver concepts are free to change. The FCM is solved again, and the change in composite risk from the baseline is recorded. Two checks are reported. The first is whether risk rises under the imposed stress. The second is whether the combined change in risk is larger or smaller than the sum of the single-stressor changes from the same baseline. A larger combined change is a superadditive response; a smaller one is subadditive. This comparison does not explain either response. Scenario results depend on both the causal model and the absolute clamp values.

3.6. Sensitivity Analysis as a Measure of Robustness

All ratings and causal weights for both the PFMEA and the FCM are hypothetical values (Section 3.7). Sensitivity analysis assesses how selected findings depend on the FCM weights and modeling constants, which represent perceived causal strengths and modeling choices based on conceptual knowledge rather than production data. Weight sensitivity is assessed with 200 Monte Carlo replicates using an illustrative perturbation range of $\pm 20\%$ to test local sensitivity around the assigned weights. For each replicate, independent uniform multipliers between 0.8 and 1.2 are applied to the nonzero causal weights, and the resulting weights are clipped to $[-1, 1]$. These perturbations preserve edge signs and leave absent edges at zero, testing changes in causal strength while keeping the network structure fixed.

Across the sensitivity analyses, we examine RPN–LIN rank agreement, the top-three intervention sets, and scenario ordering. Alongside the weight perturbations, we vary composite-risk weighting, mitigation targets, driver baselines, transfer-function steepness, and update rule one at a time while holding other settings at their reference values. Leading

candidates are assessed separately for the shared failure modes and the full intervention set. Additional checks remove selected causal links to distinguish direct-path effects from feedback in the operator-loading example. Robustness, meaning the extent to which these conclusions stay the same when the weights and model settings are changed, is interpreted only for the tested settings and candidate set. Table A4 summarizes the parameter tests, and Supplementary Material S1 provides the full settings and implementation.

3.7. Provenance of Inputs and Implementation

All numerical inputs are illustrative and were set by the authors as a demonstration of the approach; no expert panel was convened and no production data were used. Specifically, (1) the severity, occurrence, and detection ratings and the prevention and detection controls in Table A1 were assigned hypothetically following the AIAG-VDA rating tables [2] and the press-fit failure literature [41] and (2) the sixteen signed weights in Table A2 (Appendix A) were assigned hypothetically as point values on the $[-1, 1]$ scale in steps of 0.05, using a qualitative scale of weak (about 0.30), moderate (0.45 to 0.55), strong (0.60 to 0.75), and very strong (0.80 to 0.90), with the sign of each edge fixed by the mechanism in Table A2. The precise values and relative edge ordering are illustrative assumptions, not empirically justified estimates; (3) the driver baselines (0.80 and 0.20), the mitigation clamp levels (0.15 and 0.85), and the composite-risk weighting (2.5:1) are modeling constants that encode an ordering, not measured quantities. Sections 4.1–4.5 should therefore be read as a worked numerical example of the method, and Section 4.6 tests how far selected qualitative conclusions depend on these choices. The computations use a Python 3.12 script built on the PyFCM simulation engine. Supplementary Material S1 specifies the pinned library revision and provides the reproducible implementation. It uses synchronous updates, a convergence tolerance of 10^{-8} on the maximum activation change, and a 10,000-update limit that raises an error if convergence is not reached. The random generators, seeds, edge order, and clipping policy are specified in the script supplied as Supplementary Material S1.

4. Results

4.1. PFMEA

The PFMEA worksheet follows the AIAG-VDA [2] format and can be found in Appendix A. The standard sequence of structure analysis, function analysis, failure analysis, and risk analysis has been followed to provide an example of information generated from the status quo. Structure analysis decomposes the e-drive press-fit assembly cell (the process item) into its process steps and, for each step, the relevant work element drawn from the 4M categories of Man, Machine, Method, and Material. Function analysis states the intended function and the associated product or process characteristic at each of these three hierarchical levels, namely process item, process step, and work element. For each work element, failure analysis captures the failure mode together with its failure cause and the failure effect propagated to the process item. Risk analysis assigns a severity (S) to the effect, an occurrence (O) to the cause in the presence of the existing prevention controls, and a detection (D) rating given the current detection controls. In addition to mapping the resulting S, O, and D ratings to an Action Priority of Low, Medium or High using the AP lookup table, RPN is calculated alongside AP to serve as a quantifiable measure for the comparative analysis. Seven failure modes, one per PFMEA worksheet row and corresponding to the seven failure panels of Figure 3, are documented: (1) operator part-loading error (man), (2) sensor drift (machine), (3) force-window mis-setting (method), (4) press-tooling wear (machine), (5) out-of-window insertion depth (machine), (6) missed in-line detection (method), and (7) incoming supplier component variability (material). The legacy RPN is computed as $S \times O \times D$ and reported alongside the resulting Action Priority.

Consistent with the illustrative nature of the case study, the S, O, and D ratings and the listed prevention and detection controls were assigned hypothetically as plausible values for such a cell; they are not measurements from a production line and were not elicited from practitioners (Section 3.7).

4.2. FCM

These seven modes from the PFMEA were used as a framework to build the FCM. The FCM comprised twelve concepts and sixteen signed edges shown in Figure 4, with seven concepts that correspond one to one to the seven rated failure-mode rows of the PFMEA worksheet (shared) and five that have no rated row (FCM-only); the classification rule is given in the caption of Table 1, and the five FCM-only concepts are examined in Section 4.4. Maintenance budget adequacy (C8) and supplier component variability (C11) are treated as exogenous drivers clamped at a nominally normal, favorable operating point of 0.80 (medium to high influence) and 0.20 (low influence) respectively. The full edge list, with the rationale for each sign and magnitude, is given in Table A2 of Appendix A. Concept identifiers are retained from a larger candidate concept list from which the map was pruned; the gaps in the numbering carry no meaning.

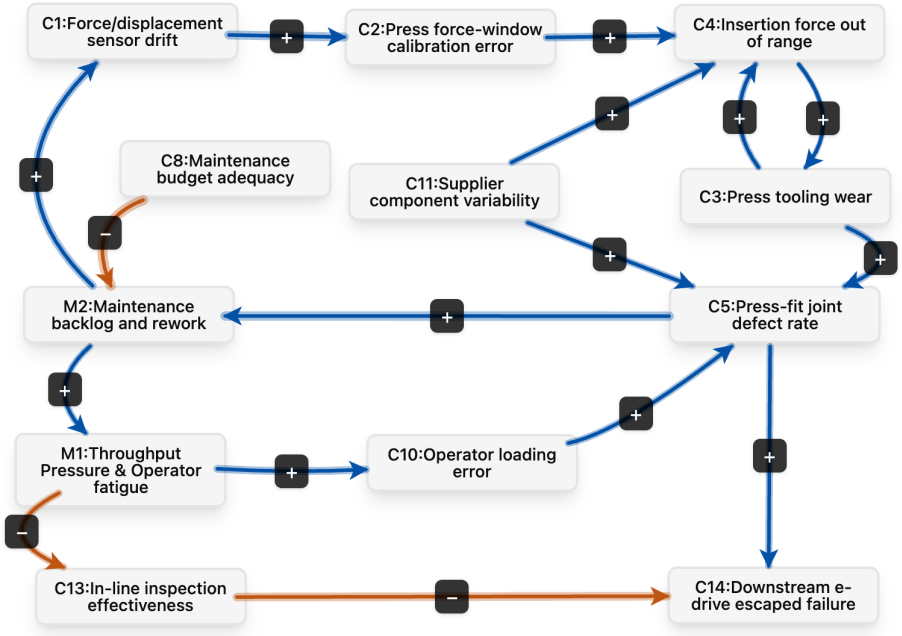


Figure 4. Fuzzy Cognitive Map for an automotive e-drive press-fit assembly cell.

M1 and M2 are composite concepts, each jointly representing two related factors (throughput pressure with operator fatigue, and maintenance backlog with rework). Bundling is a deliberate simplification adopted to keep the illustrative map small; it assumes that the two factors in each pair move together, which is plausible for a cell under schedule pressure but not guaranteed. Separating them would require additional edges and weights that this study has no basis to assign, so the split is deferred to the calibration study proposed in Section 5, where the two constructs can be elicited separately. In FCM graph theory, concepts are classified structurally as transmitters or drivers (outgoing edges only), receivers (incoming edges only), or ordinary concepts (concepts that are influenced by others but also have influence in the system) [20]. The driver, state, and outcome roles used in this study instead denote analytical functions. In this model, the baseline drivers C8 and C11 are clamped inputs and are structurally transmitters, while the concepts designated as states are structurally ordinary. The outcome concepts are those read out to calculate

composite risk. Of the two outcomes, C14 is a graph-theoretic receiver, with incoming edges only, whereas C5 is structurally ordinary because it also transmits to M2 and C14.

Under the memoryless Kosko equation, a concept with no incoming edges reverts to $f(0) = 0.5$ at the first update, so unclamped drivers would settle at the scale midpoint regardless of their initial values. For the two driver concepts in this study, the midpoint is not a healthy condition, since supplier variability is a negative-polarity quantity for which 0.5 denotes a moderate level of variation, and budget adequacy a positive-polarity quantity for which 0.5 denotes a half-adequate budget. Hence, the resulting steady state would describe a mediocre operating environment rather than business-as-usual operation. Holding the driver values constant at 0.80 and 0.20 instead anchors the baseline at the intended healthy operating point, from which the scenario analysis then imposes deviations. A practitioner should set each driver baseline to the level that describes normal operation of the cell under study (for example, the fraction of the planned maintenance budget actually released, or the incoming-inspection reject rate mapped onto the (0, 1) scale) and, as in Section 4.6, assess the sensitivity of the leverage ranking to the choice. Using the composite-risk definition in Section 3.3, the baseline is obtained by solving the model from 0.5 for all free concepts, with the stated driver clamps. Its risk is $R_0 = 1.939$. Figure 5 displays the baseline profile as a bar chart of the steady-state activations against the neutral initial value of 0.5. This provides the FCM-side counterpart of the PFMEA worksheet's initial assessment. Each concept's deviation from neutral, with the drivers held at their nominal values, constitutes the model's baseline risk snapshot under "business-as-usual" conditions.

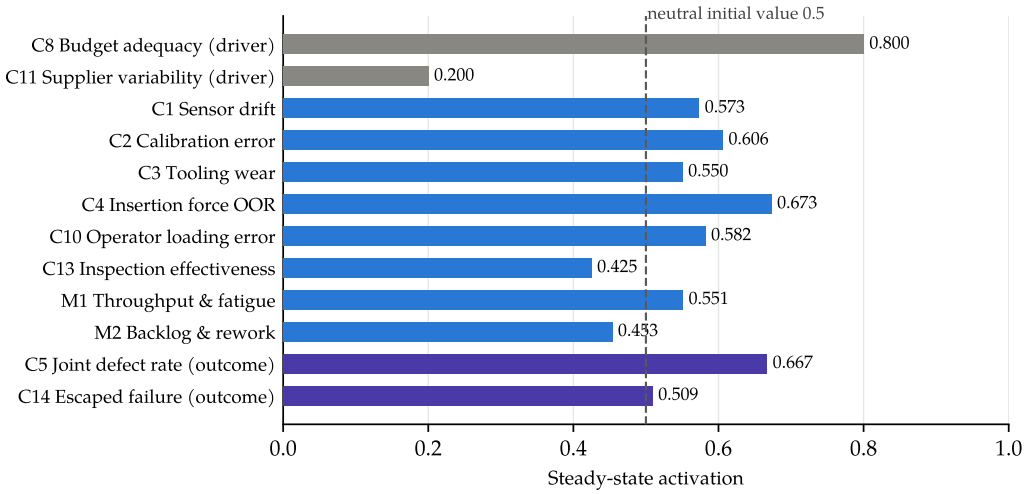


Figure 5. Baseline steady-state activations of the twelve concepts with the neutral initial value 0.5 marked; drivers are held constant at 0.80 and 0.20.

4.3. Comparison of PFMEA and FCM Leverage Points

Table 2 places the static prioritizations against FCM leverage points for the seven shared analyses. Under the AIAG-VDA table these modes resolve into five Medium (C2, C3, C4, C10, C13), and two Low (C1, C11), with no High, whereas LIN spreads them across approximately three orders of magnitude (0.01% to 9.54%). This difference serves as a demonstration of how two concepts which share a Medium rating can differ in system leverage by more than two orders of magnitude (C13 = 9.54% and C2 = 0.04%) as a result of a clear separation by the FCM. In such cases, FCM provides greater differentiation of modeled intervention leverage. Note that C11 is a clamped driver; its LIN reflects the distance from its baseline (0.20) to the mitigation clamp (0.15), see Section 3.3.

In the illustrative case study comparison, LIN retains leading RPN priorities while bringing a failure mode ranked lower by RPN into the shortlist (Table 2). This change results

from comparing individual mitigations by their modeled reduction in system-wide risk. It demonstrates how causal modeling can distinguish intervention opportunities within the same Action Priority category and, further, identify priorities for additional assessment. The priorities depend on the modeled and specified targets. Costs, feasibility, and combined effects must also be considered before the implementation of risk reduction strategies.

Link-removal "checks" examine the causal explanation for this change in priorities. Removing the tested feedback route has little effect on the modeled intervention benefit, whereas removing the direct connection to a risk outcome eliminates it. At the reference settings, the reprioritization therefore does not depend on strong amplification through that feedback relationship. Table A2 documents the causal links, and Supplementary Material S1 provides the complete link-removal results.

Figure 6 uses back-to-back bars with separate raw axes for RPN and LIN (%). The measures have different units and decision meanings; their bar lengths are not directly comparable.

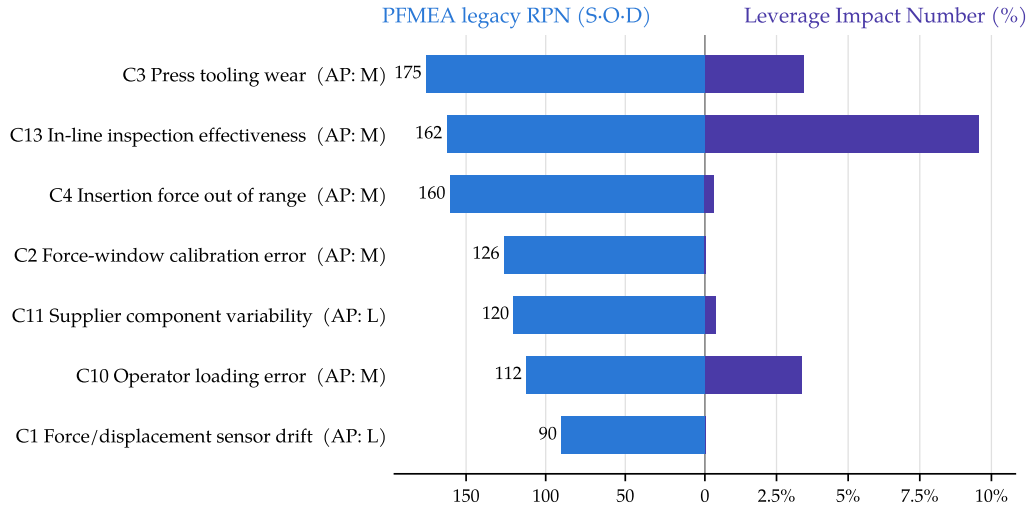


Figure 6. PFMEA legacy RPN and FCM Leverage Impact Number for the seven shared failure modes, sorted by RPN rank.

The RPN–LIN rank correlation over the seven shared modes is moderate and positive (Spearman $\rho = 0.643$; exact permutation $p = 0.069$ one-sided and 0.139 two-sided; approximate 95% confidence interval from −0.30 to 0.95). With $N = 7$ the interval is wide and includes zero, so the coefficient describes this case and is not evidence that the two methods agree in general. Excluding the driver C11 gives $\rho = 0.771$ for the six shared state concepts. The seven-mode coefficient therefore also reflects the smaller intervention distance used for C11; neither coefficient is evidence for equal-sized or equally feasible actions. Interpreted descriptively, the two rankings share the same top pair (C3, C13) and the same bottom mode (C1) and diverge mainly on C10, which the FCM promotes from sixth to a near tie for second. Action Priority places five of the seven modes in the Medium band and two in the Low band. Its correlation with LIN is approximately $\rho = 0.47$, computed as the Pearson correlation of mid-ranks with Medium ranked above Low. The shared ranks limit discrimination within the Medium band; they do not prevent calculation of a descriptive correlation.

4.4. Concepts Covered Only by the FCM Analysis

Five of the twelve FCM concepts have no rated row in the PFMEA worksheet. Table A3 (Appendix A) reports, for each of these concepts, the closest corresponding entry in Table A1

(where present), the reason it is not rated independently in this worksheet, and its causal role in the map.

Two of the five concepts are outcome concepts (C5 and C14). They appear in the PFMEA worksheet as failure-effect text and are rated only indirectly through severity. The remaining three (M1, M2, and C8) are organizational conditions. M1 corresponds to the cause entries "fatigue, time pressure" in row 1 and "Rushed inspection" in row 6. The rework component of M2 appears in the effect text of row 6, whereas maintenance backlog is not represented as a separate state in the PFMEA worksheet. C8 has no corresponding worksheet entry. M1 has a LIN of 1.68% and ranks fourth among the ten non-outcome concepts, above the shared failure modes C4, C2, and C1. It also ranks above the driver C11; however, the mitigation of C11 involves a smaller change from baseline to target (0.20 to 0.15), so this ordering is conditional on the specified intervention sizes. M2 and C8 have low LIN values at the reference operating point (0.14% and 0.01%, respectively).

4.5. Dynamic Scenarios

FCM supports conditional "what-if" analysis by clamping the selected stressor concepts (C8, C11, and M1) to prescribed values and running the model analysis again (Table 3). At the reference settings, all four degraded scenarios increase composite risk. Combined stress produces a 5.29% increase, compared with 5.38% for the sum of the three single-stressor changes, calculated from converged values before rounding. The response is therefore near-additive and slightly subadditive at the selected clamp levels. Supplier variability produces the largest single-stressor increase (4.31%), followed by throughput pressure and fatigue (1.01%) and budget decline (0.06%). This ranking describes the prescribed scenarios at the reference model settings.

Table 3. Dynamic scenario analysis relative to baseline. Composite risk is shown to three decimal places. Percentage changes, $\Delta_s = 100(R_s - R_0)/R_0$, are shown to two decimal places. Percentage changes and the additivity comparison are calculated from unrounded converged values reported in Supplementary Material S1.

Scenario	Baseline → Scenario	Composite Risk	Change from Baseline
S0 Baseline	none (C8 = 0.80, C11 = 0.20; M1 free)	1.939	0.00%
S1 Budget decline	C8: 0.80 → 0.20	1.940	+0.06%
S2 Throughput/fatigue up	M1: free (0.55) → clamped at 0.80	1.959	+1.01%
S3 Supplier variability up	C11: 0.20 → 0.80	2.023	+4.31%
S4 Combined stress	C8: 0.80 → 0.20; C11: 0.20 → 0.80; M1: clamped at 0.80	2.042	+5.29%

Figure 7 complements the aggregate results in Table 3 by showing how each imposed stress propagates through the network and changes the steady-state activation of every concept relative to baseline.

4.6. Sensitivity and Robustness

To assess sensitivity to the hypothetical weights in this study, every non-zero edge was perturbed by an independent uniform ±20% over $N = 200$ replicates. The RPN–LIN correlation remained positive, with a mean Spearman coefficient of $\rho = 0.574$ and a range of 0.464 to 0.714; these coefficients are descriptive (Section 3.4). At the reference inference specification, the three concepts $\{C13, C3, C10\}$ remained the leading levers among both the seven shared modes and all ten non-outcome concepts in all 200 replicates, and the scenario ordering was retained. These results describe stability within the tested weight perturbations. They do not establish independence from the input assumptions or isolate the contribution of the network topology.

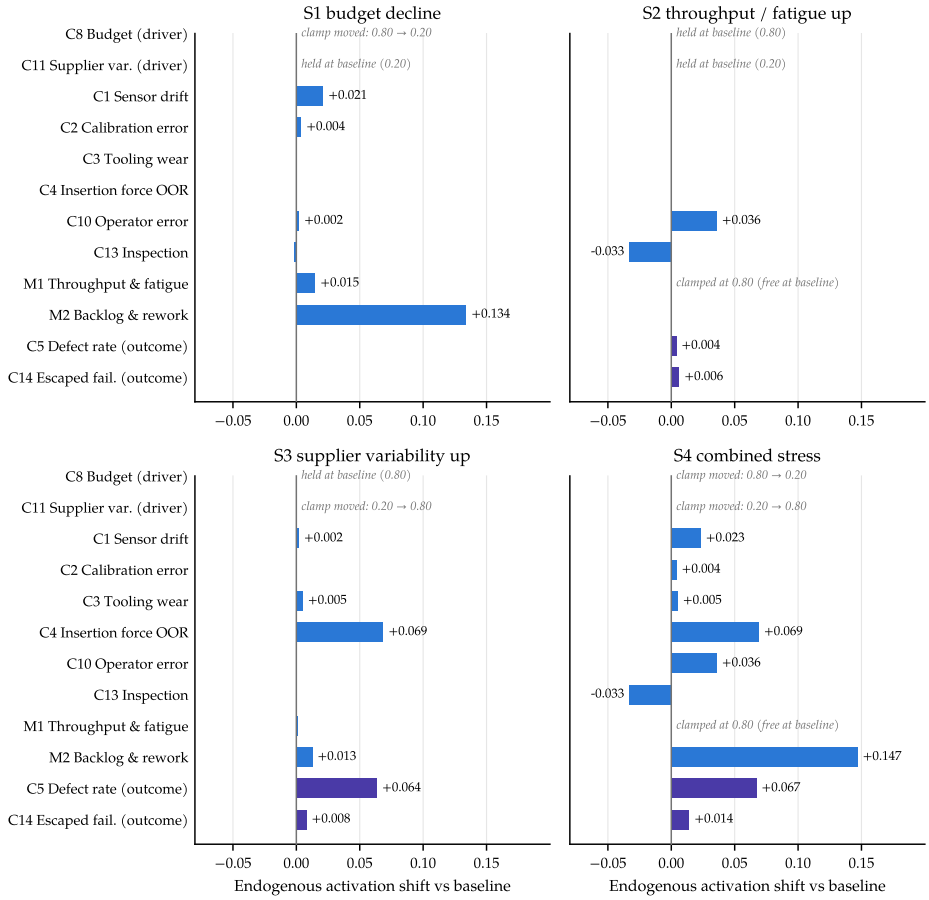


Figure 7. State-level view across all four scenarios by plotting the shift between each scenario's fixed point and the baseline steady state for every concept.

Table A4 shows that the same three shared failure modes remain the leading candidates across the tested settings, although their modeled benefits and exact ordering can change. Changing composite-risk weighting alters LIN magnitudes without changing the shared-mode order. Mitigation targets and driver baselines can affect rank agreement, partly because some absolute targets offer no improvement or worsen a driver's condition relative to its baseline. These settings test target definitions rather than beneficial mitigations. Rank exchanges between nearly tied failure modes remain after excluding the supplier-variability driver.

Inference choices have broader implications for the full intervention comparison. Higher transfer-function steepness brings organizational factors into the leading group, with alternatives for third place nearly tied at the strongest setting. The self-memory rule retains the leading sets and scenario ordering despite changes in individual ranks. Scenario ordering changes only in the most strongly saturating case ($\lambda = 5$), where the fixed target for throughput pressure and fatigue is below its level in the budget-decline scenario. Imposing that target improves this condition, so the reversal cannot be read as evidence that additional stress reduces risk. Priority stability depends on the improvement options compared and model assumptions, and intervention and scenario targets should be checked against their reference conditions.

4.7. Decision Guidance for Methodological Selection

Table 4 summarizes the study's findings into practical guidance by contrasting the three options on the factors that proved decisive here and indicating where each is best used.

Table 4. Qualitative comparison and usage guidance for PFMEA-only, FCM-only, and FCM-augmented PFMEA approaches.

Dimension	PFMEA Only	FCM Only	PFMEA + FCM
Decision criterion	AP action categories; RPN rating-based ordering	Modeled intervention effects under specified targets	AP/RPN priorities alongside modeled intervention effects
Interactions & feedback loops	No explicit propagation model	Explicit causal paths and loops	Causal model alongside the PFMEA worksheet
Systemic/ organizational factors	May appear as causes or effects; no explicit feedback model	Native concepts	Explicit causal roles alongside the PFMEA worksheet
Dynamic what-if scenarios	None (static)	Supported	Supported
Standardization & auditability	High (AIAG-VDA)	None	Retained from PFMEA
Effort & subjectivity	Low–moderate, familiar	Higher due to causal-model specification	Highest: PFMEA worksheet ratings plus causal-model assumptions
Best suited for	Compliance, localized mode-level controls, and audits	Systemic insight, intervention and scenario exploration, research	When standard compliance and quantified intervention and scenario comparisons are both required

5. Discussion

This paper compared a standards-compliant PFMEA with a Fuzzy Cognitive Map on an automotive e-drive press-fit cell and positioned the FCM as an augmentation of, not a replacement for, the PFMEA worksheet. For a process containing human–machine feedback loops and compounding degradation cycles, PFMEA assigns ratings to individual failure modes. Action Priority categories do not order modes within a band, while RPN can distinguish their isolated ratings but does not quantify propagated intervention effects. Human and organizational factors can appear in the causes section of PFMEA worksheet, but their feedback relationships and propagated intervention effects are not explicitly modeled there. The case makes these limits concrete by demonstrating how five of seven modes collapse into a single Medium band whose system Leverage Impact Number ranges from 0.04% to 9.54%, and a Medium-rated operator-error mode, ranked sixth by RPN, rises to a near tie for second when its modeled intervention effect on the outcomes is evaluated. The two orderings of the seven shared failure modes have a Spearman correlation of $\rho = 0.643$ (exact two-sided permutation $p = 0.139$). This descriptive comparison identifies agreements and differences between the decision criteria; it does not validate either representation against the process.

The augmentation of using FCM with PFMEA demonstrates three decision capabilities. First, it compares specified interventions by their effects on a common risk objective, distinguishing priorities within Action Priority bands. Second, it represents organizational conditions as connected concepts, allowing the team to evaluate potential targets that have no independent PFMEA worksheet rating. Third, it evaluates conditional scenarios, allowing the team to compare prescribed operating conditions and check whether combined stressors act approximately additively.

Rank agreement describes overlap with the PFMEA worksheet's priorities; the demonstrated value lies in examining intervention effects within Action Priority bands, organizational targets, and conditional stressor responses.

These contributions are demonstrated rather than empirically validated, and the results should be interpreted within the limits of the illustrative case. The severity, occurrence, and detection ratings and the causal weights are hypothetical values rather than measurements or panel elicitations; the composite-risk weighting of 2.5 to 1, the mitigating clamp levels of 0.15 and 0.85, and the driver baselines of 0.80 and 0.20 are modeling choices whose magnitudes carry no independent empirical claim. The comparison also rests on a single case with seven shared modes, which supports analytic rather than statistical generalization.

Two of the FCM-only concepts (M1, M2) bundle two constructs each (Section 4.2). As noted in Section 3.4, the PFMEA worksheet supplies a reference ordering for the same illustrative cell, not an independent empirical benchmark.

An FCM's behavior depends on its signed, weighted structure together with the update rule and transfer function. Previous studies show that activation-function choices can affect convergence and the accessible state space [47,48]. Among the seven shared failure modes, the top-three set is preserved across the tested inference specifications. This stability does not extend to the overall leading set: M1 enters the top three at $\lambda = 3$, and M1 and M2 do so at $\lambda = 5$, with M2 near-tied with C10 for third place. Scenario ordering is preserved at the tested steepness values up to $\lambda = 3$ and under the self-memory rule, but changes at $\lambda = 5$, where the fixed M1 stress target of 0.80 is below its free value in the budget-decline scenario. The model specification and candidate set must therefore accompany any claim about robust intervention priorities.

Future work should accordingly proceed on three fronts. The first is calibration. A suitable design is a study at a tier-1 automotive e-drive supplier covering three to five press-fit cells across two plants, so that between-cell variation in map structure can be observed. For each cell, a panel of six to ten participants (process engineer, quality engineer, maintenance lead, two operators, supplier-quality engineer) would elicit the concepts, the sign and strength of each edge, and the S, O, and D ratings in two Delphi rounds, with the inter-rater range reported for every weight and carried into the Monte Carlo analysis in place of the uniform $\pm 20\%$ band. In parallel, twelve months of manufacturing-execution and statistical-process-control data (force-signature gate results, scrap and rework counts, downtime by cause code, incoming-inspection results, and downstream escape records) would anchor the two outcome concepts and the driver baselines. Subsequent observations of specified interventions, with costs, feasibility, and concurrent production changes recorded, would test whether modeled risk reductions correspond to observed changes in defects and escaped failures. Comparing implemented interventions selected using LIN with those selected using PFMEA priorities would then assess practical decision value under comparable operating constraints. The second is replication of the comparison across multiple cells and process types to test external validity. The third is to connect the FCM to real-time or periodically updated factory data, so that the causal model can be updated alongside the retained PFMEA worksheet as operating conditions change. Pursued in that direction, the pairing of PFMEA with Fuzzy Cognitive Mapping offers a route to manufacturing risk assessment that retains the auditability of the established standard while adding the systemic, dynamic, and propagation-aware reasoning the standard alone cannot provide.

6. Conclusions

This study demonstrates a reproducible workflow that adds comparisons of intervention effects and operating scenarios to a standards-compliant PFMEA while retaining the PFMEA worksheet and its compliance artifacts. The illustrative case distinguishes intervention leverage within Action Priority bands and evaluates organizational conditions that are not independently rated in the PFMEA worksheet. Sensitivity analysis shows that the set of leading interventions among PFMEA worksheet failure modes remained unchanged across the tested assumptions, while organizational interventions became more prominent under some model settings when all candidates were considered. Scenario comparisons also depend on how stress conditions are defined, because a prescribed target does not necessarily represent an increase in stress under every model setting. These findings show why intervention priorities and scenario outcomes must be interpreted alongside the causal assumptions, candidates considered, and changes being modeled. Rank agreement identifies retained and changed priorities but does not establish more

accurate production decisions. All inputs are hypothetical and illustrative. The next step is the calibration study specified in Section 5, using practitioner input and production data to test whether predicted intervention effects correspond to observed outcomes and whether the augmented workflow improves decisions under practical constraints.

Supplementary Materials: The following supporting information can be downloaded at: https://www.mdpi.com/article/10.3390/systems14101310/s1. Supplementary Material S1: Reproducible Python analysis script, dependency requirement, execution instructions, and numerical results. The analysis code and dependencies are also publicly available at https://github.com/amin-sehati/pfmea-fcm (accessed on 27 September 2026).

Author Contributions: Conceptualization, A.S. and S.A.G.; methodology, A.S. and S.A.G.; software, A.S.; validation, A.S.; formal analysis, A.S.; investigation, A.S.; data curation, A.S.; writing—original draft preparation, A.S.; writing—review and editing, S.A.G.; visualization, A.S.; supervision, S.A.G. All authors have read and agreed to the published version of the manuscript.

Funding: This research received no external funding.

Institutional Review Board Statement: Not applicable.

Informed Consent Statement: Not applicable.

Data Availability Statement: The PFMEA ratings, causal weights, model settings, and scenario definitions are reported in the article and Appendix A. Supplementary Material S1 provides the computational implementation and complete numerical outputs, including the Monte Carlo analysis. The analysis code and dependencies are publicly available at https://github.com/amin-sehati/pfmea-fcm (accessed on 27 September 2026).

Conflicts of Interest: The authors declare no conflicts of interest.

Abbreviations

The following abbreviations are used in this manuscript:

FMEA	Failure Mode and Effects Analysis
PFMEA	Process Failure Mode and Effects Analysis
FCM	Fuzzy Cognitive Map
RPN	Risk Priority Number
AP	Action Priority
AIAG	Automotive Industry Action Group
VDA	Verband der Automobilindustrie
S, O, D	Severity, Occurrence, Detection
LIN	Leverage Impact Number
MCDM	Multi-Criteria Decision-Making
FMECA	Failure Mode, Effects and Criticality Analysis
OEM	Original Equipment Manufacturer
QMS	Quality Management System
IoT	Internet of Things
NVH	Noise, Vibration, and Harshness

Appendix A

This appendix collects the PFMEA worksheet (Table A1) and the three wide tables referenced in the main text: the signed causal weights with the rationale for each edge (Table A2), the concepts covered only by the FCM (Table A3), and the one-way sensitivity analysis of the leverage ranking (Table A4).

Table A1. PFMEA Worksheet for an automotive e-drive press-fit assembly cell.

Process Item	Process Step	Process Work Element	Function of Process Item	Function of Process Step + Product Characteristics	Function of Work Element + Process Characteristics	Failure Effect	Failure Mode	Failure Cause	S	Current Prevention Control	O	Current Detection Control	D	AP
E-drive press-fit assembly cell	Part loading	Man—operator setup	Produce conforming press-fit joints to spec	Locate components correctly with correct orientation and seating	Operator follows standard	Mislocated part	Part-loading error	Fatigue, time pressure, ambiguous work instruction	7	Loading poka-yoke	4	Orientation sensor	4	M
E-drive press-fit assembly cell	Force monitoring	Machine—position sensor	Produce conforming press-fit joints to spec	Monitor insertion force displacement	Sensor reports actual force/position	Out-of-spec joints	Slow sensor drift	Aging drift, outdated calibration	5	Scheduled load-cell calibration	3	Periodic reference-load check	6	L
E-drive press-fit assembly cell	Press setup	Method—force-range calibration	Produce conforming press-fit joint to spec	Set correct force-displacement accept window	Reference signature set correctly	Retention failure	Force displacement window mis-set	Setup error, wrong reference signature loaded	7	Recipe lock	3	Signature verification	6	M
E-drive press-fit assembly cell	Press-fit	Machine—press tooling	Produce conforming press-fit joints to spec	Drive component to seat, seat depth and retention force	Tooling within wear limit, tooling wear less than limit	Component misalignment	Press tooling wear	Abrasive or oversize parts	7	Tooling-life monitoring, scheduled service	5	Force-signature trend, post-press gauging	5	M
E-drive press-fit assembly cell	Press-fit	Machine—press process output	Produce conforming press-fit joints to spec	Insert within force/depth window	Force/depth held within window	Joint loosening/damage	Insertion depth out of window	Tooling wear, calibration drift	8	Closed-loop force control	4	In-line force-displacement signature gate	5	M
E-drive press-fit assembly cell	In-line inspection	Method—force signature inspection	Produce conforming press-fit joints to spec	Detect nonconforming joints	Low escape rate	Field failure/rework	Missed defect	Rushed inspection, sensor drift	9	Calibrated sensors, GR&R	3	Process audit, vision check	6	M
E-drive press-fit assembly cell	Incoming material	Material—components (housing, bearing, etc.)	Produce conforming press-fit joint to spec	Spec-conforming components	Incoming components within spec	Retention/NVH failure	Supplier component variability	Dimensional variation	6	Incoming inspection plan, Supplier data	4	Incoming dimensional sampling	5	L

Table A2. Signed causal weights (16 edges), assigned hypothetically as described in Section 3.7; the rationale column gives the assumed mechanism for each sign and the qualitative interpretation of each hypothetical magnitude.

From	To	Weight	Rationale
C1	C2	+0.75	A drifting sensor shifts the reference signature against which the window is set (strong).
C2	C4	+0.60	A mis-set window passes out-of-range insertions or sets wrong force targets (strong).
C3	C4	+0.45	Worn tooling changes the effective interface force (moderate).
C3	C5	+0.55	Worn tooling cocks the part and misaligns the joint (moderate).
C4	C3	+0.30	Out-of-range force accelerates tooling wear (weak).
C11	C4	+0.55	Dimensional variation changes the required insertion force (moderate).
C11	C5	+0.50	Dimensional variation directly produces interference errors (moderate).
C5	M2	+0.80	Defects create rework and consume maintenance capacity (very strong).
M2	M1	+0.45	Backlog and rework raise throughput pressure and fatigue (moderate).
M2	C1	+0.65	Deferred maintenance leaves calibration overdue and lets drift grow (strong).
C8	M2	−0.90	An adequate budget clears the backlog (very strong, negative).
M1	C10	+0.60	Time pressure and fatigue increase loading errors (strong).
M1	C13	−0.55	Rushed inspection lowers detection effectiveness (moderate, negative).
C10	C5	+0.50	Mis-loaded parts produce defective joints (moderate).
C13	C14	−0.70	Effective inspection stops defects from escaping (strong, negative).
C5	C14	+0.50	More defects mean more escapes at a given detection level (moderate).

Table A3. Concepts covered only by the FCM analysis. LIN is not reported for the two outcome concepts because they enter the composite risk directly.

ID	Concept	Role	Closest Entry in Table A1	Why It Is Not Independently Rated Here	Causal Role in the Map	LIN (%)
C5	Press-fit joint defect rate	outcome	Failure-effect text “Out-of-spec joints”, “Component misalignment”, “Joint loosening/damage”	An effect, not a failure mode; rated only indirectly through severity	Receives C3, C11, C10; feeds M2 and C14; member of both feedback loops through M2	n/a
C14	Downstream e-drive escaped failure	outcome	Failure-effect text “Field failure/rework” (row 6)	As above	Receiver of C5 (+0.50) and C13 (−0.70)	n/a
M1	Throughput pressure & operator fatigue	state	Cause text “fatigue, time pressure” (row 1) and “Rushed inspection” (row 6), unrated	A working condition affecting several rows, not a process-step failure	M2 → M1 → C10, C13; member of the defect–backlog–fatigue–error loop	1.68
M2	Maintenance backlog and rework	state	“Rework” in effect text (row 6); backlog not explicit (nearest cause: “outdated calibration”, row 2)	An organizational state, not a process-step failure	C5, C8 → M2 → M1, C1; member of both feedback loops through M2	0.14
C8	Maintenance budget adequacy	driver	None	An organizational input outside the process scope	Transmitter: C8 → M2 (−0.90)	0.01

Table A4. One-way sensitivity of the seven shared failure modes to the modeling constants and inference specification. LIN values are percentages; all other settings are held at their reference values. Values are rounded to two decimal places; 0.00 does not necessarily indicate an exactly zero effect. "Unchanged" denotes the reference shared-mode order. The top-three set $\{C13, C3, C10\}$ is retained among these seven modes in every row; this does not imply an unchanged leading set among all ten intervention candidates (Section 4.6). † marks target levels at or above C11's baseline: its zero or negative LIN is a consequence of the absolute target definition, not a beneficial mitigation. The seven-mode correlations include this definitional effect.

Setting	C13	C3	C10	C11	C4	C2	C1	Order of Shared Modes	ρ
Reference: 2.5:1, 0.15/0.85, C8 = 0.80, C11 = 0.20, $\lambda = 1$, memoryless	9.54	3.43	3.36	0.38	0.32	0.04	0.01	C13 > C3 > C10 > C11 > C4 > C2 > C1	0.643
Composite weighting 1:1	6.30	4.84	4.75	0.54	0.46	0.06	0.01	unchanged	0.643
Composite weighting 2:1	8.79	3.76	3.68	0.42	0.36	0.04	0.01	unchanged	0.643
Composite weighting 5:1	11.53	2.56	2.51	0.29	0.24	0.03	0.00	unchanged	0.643
Composite weighting 10:1	12.86	1.98	1.94	0.22	0.19	0.02	0.00	unchanged	0.643
Clamp 0.05/0.95	11.75	4.31	4.16	1.15	0.39	0.05	0.01	unchanged	0.643
Clamp 0.10/0.90	10.65	3.87	3.76	0.77	0.36	0.04	0.01	unchanged	0.643
Clamp 0.20/0.80 †	8.43	2.99	2.96	0.00	0.29	0.03	0.01	C11 falls to 7th	0.679
Clamp 0.25/0.75 †	7.32	2.55	2.56	−0.38	0.26	0.03	0.00	C10 and C3 swap; C11 7th	0.500
Clamp 0.30/0.70 †	6.20	2.12	2.17	−0.75	0.23	0.03	0.00	as above	0.500
Driver C11 = 0.10 †	9.61	3.49	3.43	−0.39	0.32	0.04	0.01	C11 falls to 7th	0.679
Driver C11 = 0.30	9.48	3.36	3.28	1.13	0.32	0.04	0.01	unchanged	0.643
Driver C11 = 0.40	9.41	3.29	3.21	1.85	0.32	0.04	0.01	unchanged	0.643
Driver C8 = 0.60 to 0.90	9.54–9.56	3.43	3.36	0.38	0.32	0.04	0.01	unchanged (no LIN moves by more than 0.02 points)	0.643
$\lambda = 0.5$	4.63	1.59	1.52	0.19	0.07	0.00	0.00	unchanged	0.643
$\lambda = 2$	19.27	6.25	6.27	0.53	1.17	0.19	0.05	C10 and C3 swap; C4 above C11	0.536
$\lambda = 3$	27.95	6.00	6.12	0.35	1.36	0.17	0.04	as above	0.536
$\lambda = 5$	39.81	1.74	1.89	0.04	0.35	0.01	0.00	as above; scenario order lost	0.536
Self-memory update rule	6.55	2.87	2.80	0.20	0.24	0.02	0.00	C4 above C11	0.714

References

1. Rausand, M.; Høyland, A. *System Reliability Theory: Models, Statistical Methods, and Applications*, 2nd ed.; Wiley: Hoboken, NJ, USA, 2004.
2. AIAG (Automotive Industry Action Group); VDA (Verband der Automobilindustrie). *Failure Mode and Effects Analysis (FMEA) Handbook*, 1st ed.; Automotive Industry Action Group: Southfield, MI, USA; Verband der Automobilindustrie: Berlin, Germany, 2019.
3. Pantazopoulos, G.; Tsinopoulos, G. Process failure modes and effects analysis (PFMEA): A structured approach for quality improvement in the metal forming industry. *J. Fail. Anal. Preven.* **2005**, *5*, 5–10. [CrossRef]
4. Ben-Daya, M. Failure Mode and Effect Analysis. In *Handbook of Maintenance Management and Engineering*; Ben-Daya, M., Duffuaa, S., Raouf, A., Knezevic, J., Ait-Kadi, D., Eds.; Springer: London, UK, 2009. [CrossRef]
5. *ISO 13485:2016*; Medical Devices—Quality Management Systems—Requirements for Regulatory Purposes. International Organization for Standardization: Geneva, Switzerland, 2016.
6. Bills, E.; Mastrangelo, S.; Wu, F. Documenting Medical Device Risk Management through the Risk Traceability Summary. *Biomed. Instrum. Technol.* **2015**, *49*, 26–33. [CrossRef] [PubMed]
7. Johnson, K.G.; Khan, M.K. A study into the use of the process failure mode and effects analysis (PFMEA) in the automotive industry in the UK. *J. Mater. Process. Technol.* **2003**, *139*, 348–356. [CrossRef]
8. ElMaraghy, H.; Monostori, L.; Schuh, G.; ElMaraghy, W. Evolution and future of manufacturing systems. *CIRP Ann.* **2021**, *70*, 635–658. [CrossRef]
9. Liu, H.C.; Liu, L.; Liu, N. Risk evaluation approaches in failure mode and effects analysis: A literature review. *Expert Syst. Appl.* **2013**, *40*, 828–838. [CrossRef]
10. Liou, J.J.H.; Guo, B.H.T.; Huang, S.-W.; Yang, Y.-T. Failure mode and effect analysis using interval type-2 fuzzy and multiple-criteria decision-making methods. *Mathematics* **2024**, *12*, 3931. [CrossRef]

11. Magalhães, W.R.d.; Lima Junior, F.R. A model based on FMEA and Fuzzy TOPSIS for risk prioritization in industrial processes. *Gestão Prod.* **2021**, *28*, e5535. [CrossRef]
12. Shao, J.; Zhong, S.; Tian, M.; Liu, Y. Combining fuzzy MCDM with Kano model and FMEA: A novel 3-phase MCDM method for reliable assessment. *Ann. Oper. Res.* **2024**, *342*, 725–765. [CrossRef]
13. United States Department of Defense. *MIL-P-1629: Procedures for Performing a Failure Mode, Effects and Criticality Analysis*; Department of Defense: Washington, DC, USA, 1949.
14. Banduka, N.; Petrovic, T.; Komatina, N. Model for the Assessment of Process Failure Mode and Effect Analysis Maturity Level in the Automotive Industry toward Industry 4.0 Trends. *Int. Rev.* **2024**, 219–228. [CrossRef]
15. Thomas, D. Rethinking FMEA for Today's Manufacturing Landscape Considering Innovation in Risk Analysis. *J. Fail. Anal. Preven.* **2025**, *25*, 1–3. [CrossRef]
16. Ivanov, D.; Dolgui, A.; Sokolov, B. The impact of digital technology and Industry 4.0 on the ripple effect and supply chain risk analytics. *Int. J. Prod. Res.* **2019**, *57*, 829–846. [CrossRef]
17. Di Nardo, M.; Murino, T.; Pandey, S. A Failure Mode and Effects Analysis (FMEA) risk assessment template for collaborative robot. *Proc. Inst. Mech. Eng. Part O J. Risk Reliab.* **2026**, *in press*. [CrossRef]
18. Nguyen, D.-T.; Duong, Q.B.; Zamai, E.; Shahzad, M.K. Fault diagnosis for the complex manufacturing system. *Proc. Inst. Mech. Eng. Part O J. Risk Reliab.* **2016**, *230*, 178–194. [CrossRef]
19. Kosko, B. Fuzzy cognitive maps. *Int. J. Man-Mach. Stud.* **1986**, *24*, 65–75. [CrossRef]
20. Özesmi, U.; Özesmi, S.L. Ecological models based on people's knowledge: A multi-step fuzzy cognitive mapping approach. *Ecol. Model.* **2004**, *176*, 43–64. [CrossRef]
21. Gray, S.A.; Gray, S.; De Kok, J.L.; Helfgott, A.E.R.; O'Dwyer, B.; Jordan, R.; Nyaki, A. Using Fuzzy Cognitive Mapping as a Participatory Approach to Analyze Change, Preferred States, and Perceived Resilience of Social-Ecological Systems. *Ecol. Soc.* **2015**, *20*, 11. [CrossRef]
22. Jetter, A.J.; Kok, K. Fuzzy cognitive maps for futures studies—A methodological assessment of concepts and methods. *Futures* **2014**, *61*, 45–57. [CrossRef]
23. Gray, S.; Chan, A.; Clark, D.; Jordan, R. Modeling the integration of stakeholder knowledge in social–ecological decision-making: Benefits and limitations to knowledge diversity. *Ecol. Model.* **2012**, *229*, 88–96. [CrossRef]
24. Azadegan, A.; Porobic, L.; Ghazinoory, S.; Samouei, P.; Saman Kheirkhah, A. Fuzzy logic in manufacturing: A review of literature and a specialized application. *Int. J. Prod. Econ.* **2011**, *132*, 258–270. [CrossRef]
25. Wong, B.K.; Lai, V.S. A survey of the application of fuzzy set theory in production and operations management: 1998–2009. *Int. J. Prod. Econ.* **2011**, *129*, 157–168. [CrossRef]
26. Bowles, J.B.; Peláez, C.E. Fuzzy logic prioritization of failures in a system failure mode, effects and criticality analysis. *Reliab. Eng. Syst. Saf.* **1995**, *50*, 203–213. [CrossRef]
27. Stylios, C.D.; Groumpos, P.P. Fuzzy cognitive maps: A model for intelligent supervisory control systems. *Comput. Ind.* **1999**, *39*, 229–238. [CrossRef]
28. Stylios, C.D.; Groumpos, P.P. The challenge of modelling supervisory systems using fuzzy cognitive maps. *J. Intell. Manuf.* **1998**, *9*, 339–345. [CrossRef]
29. Bertolini, M.; Bevilacqua, M. Fuzzy cognitive maps for human reliability analysis in production systems. In *Production Engineering and Management under Fuzziness*; Kahraman, C., Yavuz, M., Eds.; Springer: Berlin/Heidelberg, Germany, 2010; pp. 381–415. [CrossRef]
30. Stylios, C.D.; Groumpos, P.P. Modeling complex systems using fuzzy cognitive maps. *IEEE Trans. Syst. Man Cybern. A* **2004**, *34*, 155–162. [CrossRef]
31. Papageorgiou, E.I.; Salmeron, J.L. A review of fuzzy cognitive maps research during the last decade. *IEEE Trans. Fuzzy Syst.* **2013**, *21*, 66–79. [CrossRef]
32. Felix, G.; Nápoles, G.; Falcon, R.; Froelich, W.; Vanhoof, K.; Bello, R. A review on methods and software for fuzzy cognitive maps. *Artif. Intell. Rev.* **2019**, *52*, 1707–1737. [CrossRef]
33. Salmeron, J.L.; Gutierrez, E. Fuzzy Grey Cognitive Maps in reliability engineering. *Appl. Soft Comput.* **2012**, *12*, 3818–3824. [CrossRef]
34. Bakhtavar, E.; Valipour, M.; Yousefi, S.; Sadiq, R.; Hewage, K. Fuzzy cognitive maps in systems risk analysis: A comprehensive review. *Complex Intell. Syst.* **2021**, *7*, 621–637. [CrossRef]
35. Jahangoshai Rezaee, M.; Yousefi, S.; Babaei, M. Multi-stage cognitive map for failures assessment of production processes: An extension in structure and algorithm. *Neurocomputing* **2017**, *232*, 69–82. [CrossRef]
36. Jahangoshai Rezaee, M.; Yousefi, S.; Valipour, M.; Dehdar, M.M. Risk analysis of sequential processes in food industry integrating multi-stage fuzzy cognitive map and process failure mode and effects analysis. *Comput. Ind. Eng.* **2018**, *123*, 325–337. [CrossRef]
37. Yousefi, S.; Jahangoshai Rezaee, M.; Moradi, A. Causal effect analysis of logistics processes risks in manufacturing industries using sequential multi-stage fuzzy cognitive map: A case study. *Int. J. Comput. Integr. Manuf.* **2020**, *33*, 1055–1075. [CrossRef]

38. Abbaspour Onari, M.; Yousefi, S.; Jahangoshai Rezaee, M. Risk assessment in discrete production processes considering uncertainty and reliability: Z-number multi-stage fuzzy cognitive map with fuzzy learning algorithm. *Artif. Intell. Rev.* **2021**, *54*, 1349–1383. [CrossRef]
39. Alruqi, M.; Baumers, M.; Branson, D.T.; Girma, S. The challenge of deploying failure modes and effects analysis in complex system applications—Quantification and analysis. *Sustainability* **2022**, *14*, 1397. [CrossRef]
40. Peláez, C.E.; Bowles, J.B. Using fuzzy cognitive maps as a system model for failure modes and effects analysis. *Inf. Sci.* **1996**, *88*, 177–199. [CrossRef]
41. You, B.; Lou, Z.; Luo, Y.; Xu, Y.; Wang, X. Prediction of pressing quality for press-fit assembly based on press-fit curve and maximum press-mounting force. *Int. J. Aerosp. Eng.* **2015**, *2015*, 823019. [CrossRef]
42. Harmati, I.Á.; Kóczy, L.T. On the Convergence of Input-Output Fuzzy Cognitive Maps. In *Rough Sets: International Joint Conference, IJCRS 2020, Havana, Cuba, 29 June–3 July 2020, Proceedings*; Springer: Cham, Switzerland, 2020; Volume 12179, pp. 449–461. [CrossRef]
43. Mkhitaryan, S.; Giabbanelli, P.; Wozniak, M.K.; Nápoles, G.; De Vries, N.; Crutzen, R. FCMpy: A python module for constructing and analyzing fuzzy cognitive maps. *PeerJ Comput. Sci.* **2022**, *8*, e1078. [CrossRef] [PubMed]
44. Glevitzky, M.; Popa, M.; Mucea-Ştef, P.; Popa, D.M. A risk management approach in occupational health and safety based on the integration of a weighted composite score. *Safety* **2025**, *11*, 103. [CrossRef]
45. de Winter, J.C.F.; Gosling, S.D.; Potter, J. Comparing the Pearson and Spearman correlation coefficients across distributions and sample sizes: A tutorial using simulations and empirical data. *Psychol. Methods* **2016**, *21*, 273–290. [CrossRef] [PubMed]
46. Bonett, D.G.; Wright, T.A. Sample size requirements for estimating Pearson, Kendall and Spearman correlations. *Psychometrika* **2000**, *65*, 23–28. [CrossRef]
47. Revay, P.; Giabbanelli, P.; Gray, S. Connecting Modeling Requirements and the Choice of Activation Functions in Fuzzy Cognitive Map Simulations. *Neural Comput. Appl.* **2026**, *38*, 86. [CrossRef]
48. Bueno, S.; Salmeron, J.L. Benchmarking main activation functions in fuzzy cognitive maps. *Expert Syst. Appl.* **2009**, *36*, 5221–5229. [CrossRef]

Disclaimer/Publisher's Note: The statements, opinions and data contained in all publications are solely those of the individual author(s) and contributor(s) and not of MDPI and/or the editor(s). MDPI and/or the editor(s) disclaim responsibility for any injury to people or property resulting from any ideas, methods, instructions or products referred to in the content.